Egypt. J. Chem. **Vol. 66**, No. SI: 13 pp. 1597 - 1608 (2023)

Egyptian Journal of Chemistry

http://ejchem.journals.ekb.eg/

Preparation of Aluminum Sulfate from Saudi Kaolin by Acid Treatment and its Application as a Flocculant for Surface Water Treatment Word

MA Tantawy[a,b,*], Hassen Harzali[a,c] and Abdulaziz A Alomari[a]

[a] *Chemistry Department, Faculty of Science and Arts, Mukhwah, Al-Baha University, KSA*
[b] *Chemistry department, Faculty of Science, Minia University, Egypt*
[c] *Applied Mineral Chemistry Laboratory (LR19ES02), Department of Chemistry, Faculty of Sciences of Tunis, Tunis El Manar University, Campus Universitaire Farhat Hached, 2092, Tunis, Tunisia*
** Corresponding author, mail: mohamedahmed@mu.edu.eg*

Abstract

This research aims to test the use of aluminum sulfate prepared from kaolin from Nawan, Al Baha, KSA, in the treatment of the surface water of the Al Ahsaba Dam. The analyses proved that the kaolin sample was pure and was successfully converted to amorphous metakaolin by calcination at 800 °C. Approximately 60% of alumina was extracted from metakaolin by dissolving hydrochloric and nitric acids separately. Aluminum sulfate was also separated from alumina dissolved in acids and its chemical composition was determined by analysis. The chemical changes that occurred in kaolin after calcination and in metakaolin after dissolution with acids were traced using different analytical techniques, such as TGA, XRD, FTIR, and SEM-EDX. Aluminum sulfate was used as a coagulant in the water of the Al Ahsaba dam to remove suspended solids. The chemical properties of the Al Ahsaba dam water were also tested before and after adding the prepared and industrial aluminum sulfates, such as turbidity, residual aluminum, hardness, electrical conductivity, and total dissolved solids, and compared to a sample of commercial drinking water. The results showed that aluminum sulfate prepared from kaolin Nawan is suitable for use in dam water treatment as a coagulant to remove suspended solids to supply treatment plants with the water needed to complete other treatment processes.

Keywords: Kaolin; aluminium sulphate; acid treatment; flocculant; water treatment.

1. Introduction

The kingdom of Saudi Arabia is classified by the United Nations as a water-scarce nation and sits below the severe water scarcity threshold of 500 cubic meters per capita per year by the value of 89.5 cubic meters per capita per year [1] because Saudi Arabia is in an arid region (Lat. 16.5–32.5 N; Lon. 33.75-56.25 E) with low average annual rainfall (average annual rainfall of less than 150 mm in most of the country) [2]. Approximately 60% of the rainfall occurs in the western parts of the Kingdom, while the remaining 40% occurs far south of the western coast (Tahama) [3]. Hence, the intense rainfall in the southern and southwestern regions may support better management of rainwater in these regions to deal with future water demands. The water demands in the kingdom are satisfied in the following descending order: nonrenewable groundwater sources, renewable surface and groundwater sources, desalinated water, and treated wastewater [4]. It is estimated that 65% of water comes from nonrenewable sources, while renewable sources represent only 35%. These data indicate the seriousness of the current and future water situation in the Kingdom of Saudi Arabia unless firm decisions are made and implemented to reduce unfair water

*Corresponding author e-mail: mohamedahmed@mu.edu.eg.; (MA Tantawy).
EJCHEM use only: Received date 19 January 2023; revised date 19 July 2023; accepted date 17 August 2023
DOI: 10.21608/EJCHEM.2023.188485.7480

waste and develop an integrated plan to conserve water resources in sustainable ways [5].

The total internal renewable water resources in Saudi Arabia have been estimated to be approximately 2.4 billion cubic meters BCM/year [6]. Water sources in Saudi Arabia are limited and can be affected by future climatic changes [7]. The total population of Saudi Arabia was approximately 34.2 million in mid-2019, resulting in a significant increase in water use [8]. Sustainable water resource management strategies must be implemented in a manner that rationalizes water consumption and secures its supply for future generations. The high annual population growth rate (2.5% per year) and increase in the demand for water (8.8% per year) will have a significant impact on the future availability and quality of water resources in Saudi Arabia [9]. To facilitate the storage and utilization of surface water in the Al Baha district, 40 dams were constructed [10] to store ≈ 40.76 MCM of surface runoff annually [4]. Of these, 26 recharge dams store ≈ 9.76 MCM/year of water used to recharge groundwater. Ten dams store ≈ 30.5 MCM of water annually for drinking water supply purposes (≈ 10% of the total stored drinking water in KSA). Three control dams were used to direct the water in the desired directions. One irrigation dam store 0.5 MCM water annually is used for agricultural purposes [11].

Saudi Arabia's drinking water consumption was 3.39 billion cubic meters in 2018. Desalinated water accounted for 2.14 billion cubic meters (63%) of the distributed water, while groundwater represented 1.26 billion cubic meters (37%). The drinking water consumption of Al Baha Province is 32 million cubic meter. Households consumed nearly 26.88 million cubic meters of drinking water in Al Baha Province, representing 84% of the total consumption, whereas commercial consumption accounted for just 16%. [12]. The number of domestic water connection subscribers in Al Baha Province was 45000, covering 71% of the population in 2020 [13]. The need for potable water in many small cities and villages in the Al Baha district opens the door for point-of-use household water treatment in addition to the treatment of dam water. Recent studies on rapidly emerging technologies have shown that some of these technologies are feasible and economic, while others still need more research and development.

Kaolin and clay are common weathering products of many tropical and subtropical soils and consist of the kaolinite mineral $A1_2Si_2O_5(OH)_4$ [14]. Large amounts of kaolinitic clays are widespread in clastic Phanerozoic rocks of Saudi Arabia. Kaolinitic clay has important industrial applications such as paper coating, fillers in plastics, petroleum, ceramics, porcelain, and refractories [15]. The utilization of various Saudi kaolinitic clay deposits has been investigated for various applications by many researchers. The Jabal Shahbah kaolin deposits southeast of Al Kharj were investigated to replace imported kaolin and could be utilized as a raw material for the ceramic, refractory, and filler industries in the local Saudi market [16]. Jeddah and Madina clays were found to be suitable for use in the production of ceramics and building bricks [17]. Saudi kaolin has been utilized for the production of geopolymer coating materials with promising properties [18]. The adsorption process is one of the tools used in the treatment and separation of pollutants, such as heavy metals from wastewater, with the application of low-cost adsorbents such as activated clay [19, 20]. Khulays clay, north of Jeddah, was assessed for its use as an adsorbent for the removal of Ag-(I) and Cu-(II) ions from aqueous solutions [21]. Al Shammar Mountain kaolin in Medina was found to be suitable for the adsorption of pyrrole and the catalytic conversion of methyl butanol [22]. An enormous stock of whitish kaolin deposits is located southeast of Nawan, Al Baha, covering an area of up to 10 km^2 as subsurface layers covered with sand and marl deposits and forming a large number of prominent divergent tongues [23]. Alum $Al_2(SO_4)_3.14\text{-}27H_2O$ is a coagulant that is used in water treatment plants to remove unwanted materials to provide the community with a need for safe domestic and industrial water to provide the community with a need for a safe and domestic water supply [24, 25]. Alum is traditionally extracted from bauxite, an aluminosilicate mineral, using the Bayer process [26]. Because bauxite is not found in Saudi Arabia in economic quantities [27], kaolin has been processed to produce an alum alternative to bauxite [28]. Saudi kaolin has been investigated for the production of liquid alum to satisfy the local demands of alum [29], as well as alumina [27, 30]. Nawan kaolin was utilized for the production of alumina by leaching with sulfuric acid with a recovery percentage of 67% [23]. In addition, large amounts of clay deposits were found at various locations in Al Baha District. Al Baha clay was evaluated to be used for the removal of Co^{2+} ions from wastewater after activation by NaCl [31].

This research aims to beneficiate the deposits of kaolin southeast of Nawan in the Al Baha district to produce alum and to test the suitability of alum for use in dam water treatment as a coagulant to remove suspended matter. The main objective of this research is to provide water treatment plants with an additional water source other than groundwater that is for completing treatment processes to produce healthy drinking water.

2. Materials and experimental methods

Kaolin (K) was provided from southeastern Nawan, Al Baha, KSA (19°29'10.27" N and 41°15'20.27" E) (Figure 1). Kaolin was ground to a fineness of less than 150 microns. It was incinerated at 800 °C for two hours and cooled in an oven to the laboratory temperature. The resulting metakaolin was ground to a fineness of less than 100 µm.

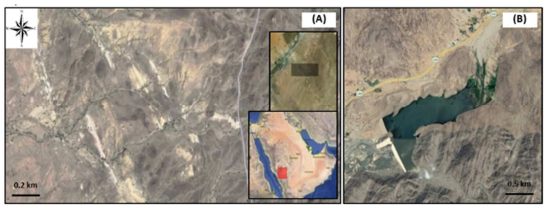

Figure 1: Map of the Kaolin location (A) and Al Ahsaba dam (B).

Metakaolin was dissolved in 8 M hydrochloric or nitric acid at a ratio of 50 g metakaolin to 500 mL of acid (acid kaolin 250%) in a round flask connected to a condenser and heated to boiling, and the mixture was stirred at 400 rpm for 2 h. Filtering was performed using a Buchner funnel and the undissolved residue was washed with distilled water and dried at 100 °C. The dissolved Al and Fe in the filtrate were determined using gravimetric analysis.

The acid-dissolving filtrate was heated to near the boiling point, and sodium hydroxide solution 10 was added until white aluminium hydroxide and reddish-brown iron hydroxide began to precipitate at pH 4-5. The iron hydroxide precipitate was separated by increasing the addition of sodium hydroxide to pH 11-12, where aluminium hydroxide was converted to soluble sodium meta-aluminate. The solution was heated to a boil and left overnight (12 h) to stabilize the iron hydroxide precipitate and facilitate filtration. After filtration, the precipitate was washed with distilled water.

Aluminium hydroxide was precipitated from the filtrate by adding an acidic solution to pH 4-5. The solution was heated to boiling temperature. The obtained solution was left overnight to stabilize the aluminium hydroxide precipitate and facilitate the filtration process. After filtration, the precipitate was washed with distilled water. Concentrated sulfuric acid was added to the final precipitate, which was stirred using a magnetic stir bar at 400 rpm. The precipitate was then completely dissolved. The resulting solution was heated for a while (estimation of time, for example, 60 min) to concentrate it. Excess of methanol was added to the saturated solution, which was then cooled in an ice bath. The aluminium sulfate crystals were separated from the solution by filtration, washed with methanol, and dried at 50 °C for 2 h. The number of hydrated water molecules and molecular formula of the prepared aluminium sulfate were calculated by gravimetric analysis.

A sample of water from the Al Ahsaba dam was brought, its pH was measured and it was packed into two 20-liter polyethylene bottles. The turbidity of the water sample was measured, and the leaching process was carried out with aluminium sulfate within 8 h of sample collection.

The prepared and commercial aluminum sulfate were used in the coagulation and liquefaction tests of the Al Ahsaba dam water sample by adding different doses of 10-40 parts per million aluminum sulfate to the water according to the method described in reference [25], and the coagulated particles were filtered. The following measurements were made on the treated water: turbidity measurement, residual aluminum concentration measurement, temporary, permanent, and total hardness measurement, temperature, pH, electrical conductivity, and total dissolved solids content. Turbidity was measured using a PD-303S spectrophotometer (APEL, Japan) at a wavelength of 860 nm using a plank sample of turbidity-free, deionized, and deionized water as a reference sample. The residual aluminum concentration was measured with EDTA solution at pH 7-8 with ammonia solution and Eriochrome black-T indicator and titrated with zinc sulfate solution according to a previously described method [32]. The temporary hardness of the water samples was measured by titration with hydrochloric acid using an orange methyl index. The total hardness of the water samples was measured by titration with EDTA solution using the Eriochrome black-T indicator and buffered ammonia pH=10. Permanent hardness was measured by subtracting the temporary hardness from the total hardness. The electrical

conductivity and total dissolved soild content of the water were measured using a calibrated electrical conductivity meter (EC 215 HANNA). The pH of the water was measured using a pH 212 microprocessor pH meter (HANNA Instruments). Figure (2) shows the kaolin location, acid treatment of metakaolin, separation of aluminum sulfate, and prepared aluminum sulfate. Figure (3) shows the sample of water from the Al Ahsaba dam, determination of residual aluminum and total hardness, electrical conductivity meter, and turbidity measurement.

Figure 2: Kaolin location (A), acid treatment of metakaolin (B), separation of aluminum sulfate (C), and prepared aluminum sulfate (D).

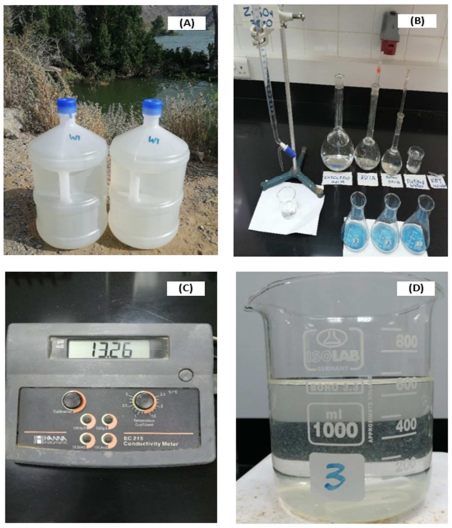

Figure 3: Water sample from Al Ahsaba dam (A), determination of residual aluminum and total hardness (B), electrical conductivity meter (C), and turbidity measurement (D).

3. Results and discussion

The content of the oxides of both Kaolin and kaolin calcined at 800 °C inferred by XRF analysis (Table 1) shows that K contains 37.90 wt% Al_2O_3, 46.21 wt% SiO_2, 1.24 wt% TiO_2, 1.79 wt% Fe_2O_3, and a 10.6 wt% loss of ignition due to the loss of chemically combined water during crystallization, as well as trace amounts of CaO, MgO, Na_2O, and K_2O oxides. Kaolin calcined at 800 °C contains 42.13 wt% Al_2O_3, 51.33 wt% SiO_2, 1.27 wt% TiO_2, 1.82 wt% Fe_2O_3, and trace amounts of CaO, MgO, Na_2O, and K_2O oxides. Assuming that the loss on ignition is only due to the loss of crystallization water from kaolin crystals, this result proves that the purity of kaolin reaches approximately 76 percent. The results for the K and MK contents were in agreement. The data obtained are not significantly different from the data for pure kaolin according to the theory of the composition of SiO_2 and Al_2O_3, which are 46% and 40%, respectively.

Table 1: XRF analysis of kaolin and kaolin calcined at 800 °C.

Oxide, Wt %	Kaolin (K)	Metakaolin (MK)
SiO_2	46.21	51.33
Al_2O_3	37.90	42.13
CaO	0.55	0.57
Fe_2O_3	1.79	1.82
MgO	0.28	0.30
SO_3	0.21	0.23
Na_2O	0.19	0.22
K_2O	0.48	0.50
TiO_2	1.24	1.27
Cl^-	0.065	0.07
LOI	10.6	1.42
Total	**99.52**	**99.86**

The XRD patterns of kaolin and kaolin calcined at 250-800 °C are shown in Figure (4). Significant peaks are observed of kaolinite. These results indicate that kaolin is mainly composed of kaolinite ($Al_2O_3.2SiO_2.2H_2O$) and quartz (SiO_2). The diffraction pattern of MK800 (kaolin calcined at 800 °C) is distinct from the diffraction patterns of MK500 and MK250 (kaolin calcined at 250 and 500 °C) due to the disappearance of the kaolin peaks. This proves that the heat treatment before 800 °C did not complete the dehydration of the hydroxyl groups.

However, at the end of the heat treatment at 800 °C, hydroxyl groups were removed. The produced metakaolin consisted of amorphous anhydrous aluminum silicate and quartz phases, which remained unaffected by heating at 800 °C. The sample become completely amorphous at 800 °C, with no evidence of γ-alumina formation. This confirms that 800 °C is suitable for the preparation of metakaolin from kaolin. The hump attributed to amorphous metakaolin disappeared after treatment of metakaolin with acids (MKRH and MKRN). This confirmed that it was attributed to amorphous alumina, which was dissolved in acids. However, the residual amorphous silica did not exhibit a hump in the XRD analysis. The most characteristic peaks for potassium alum ($KAl(SO_4)_2{\cdot}12H_2O$) appeared at 20.6, 22, 24.6, 27,4 and 32.2 in case of ASN, and those for tamarugite ($NaAl(SO_4)_2{\cdot}6H_2O$) appeared at 21, 22.4, 24.4, 28.2, and 30.8 in case of ASH [33]. The appearance of a hump in the case of aluminum sulfate confirms that the material is not well crystallized and contains amorphous material because of the rapid precipitation of solid aluminum sulfate from the solution during separation.

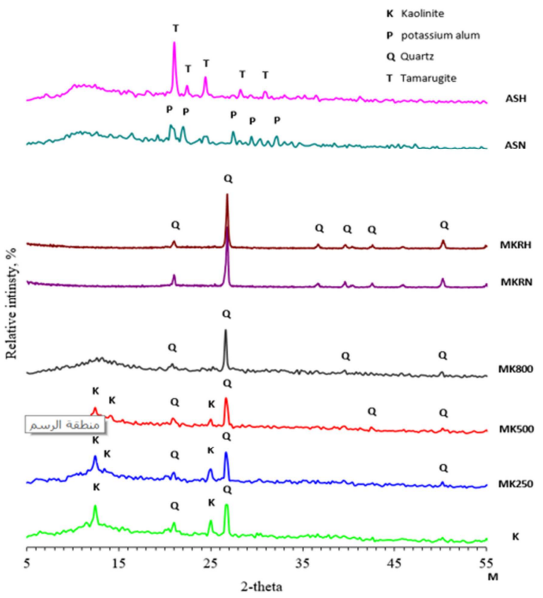

Figure 4: XRD patterns of kaolin and kaolin calcined at 250-800 °C (MK250-800), metakaolin residue after dissolution with nitric and hydrochloric acids (MKRN and MKRH), and aluminum sulfate prepared from the dissolution of metakaolin with acids (ASN and ASH).

FTIR analysis was applied to characterize the changes that occurred upon calcination of kaolin, which is an important step in the preparation of aluminum sulfate from raw kaolin. The results of the FTIR analysis of K (Figure 5) were consistent with the XRD results, confirming that kaolin contained kaolinite and quartz. Vibration bands appearing at 532, 908, 1025, 1077, 3618, and 3685 cm^{-1} are attributed to the functional groups of the kaolinite structure [34, 35]. The bands appearing at 465 and 683 cm^{-1} are attributed to the functional groups of the quartz structure [36]. The bands appearing at 1609 and 3407 cm^{-1} were attributed to the functional groups of the adsorbed water [37]. The band at 1070 cm^{-1} was is attributed to the amorphous SiO_2 group of metakaolin [38]. The band appearing at 465 cm^{-1} attributed to the vibration of O-Si-O of quartz, shifted to a lower wavenumber with increasing heat treatment of metakaolin. The characteristic bands of kaolinite completely disappeared at 800 °C. Characteristic bands of quartz and metakaolinite appeared at 800 °C. Bands appearing at 1609 and 3407 cm^{-1}, attributed to the adsorbed water, appeared after the acid treatment of metakaolin because of the adsorption of water by amorphous SiO_2 [38]. The band appearing at 3407 cm^{-1}, attributed to the water adsorbed by amorphous SiO_2, was higher in the case of nitric acid treatment (MKRN). This was related to the higher amount of amorphous silica. In the case of the prepared aluminum sulfate, the bands appearing at 1121 and 994 cm^{-1} correspond to SO_4 vibrations. The band at 593 cm^{-1} is attributed to the Al–O stretching and bending vibrational modes [39, 40]. The broad bands at 2906 and 3348 cm^{-1} are due to the OH stretching of molecular water, and the broad band at 1635 cm^{-1} is due to the OH bending of free water, revealing that the extracted salt is hydrated. The characteristic sharp sulfate (SO_4^{2-}) peaks at 468-471 cm^{-1}, 603–608 cm^{-1}, 657–686 cm^{-1}, 1104-1115 cm^{-1}, and 1237–1247 cm^{-1} correspond to the symmetrical bending mode of SO_4^{2-} degeneration of asymmetric bending, symmetrical bending, degenerate symmetric stretching, and degenerate asymmetric stretching, respectively [41].

The SEM micrographs of kaolin and kaolin calcined at 250-800 °C (Figure 6) were obtained using EDX analysis. The SEM image of kaolin was obtained at high magnification to show flat hexagonal platelets of kaolinite stacked together (Figure 6-K). The SEM images of kaolin in Figure (6) show plate-

like layers stacked over one another, confirming the morphological characteristics of kaolin clay, as previously reported. The assemblage of plate-like hexagonal structures or book-like kaolinite stacks is a common feature of kaolin clay observed under SEM. The SEM micrographs illustrate the change in the particle size and specific surface area of the produced MK owing to the calcination effect. At the beginning of calcination, the kaolinite particles contracted due to the loss of water, giving MK a smaller particle size and higher specific surface area (Figure 6-MK250-500). The absence of a clear change in the morphology of kaolin during the calcination stages at 250 and 500 °C can be explained by the fact that the kaolin structure did not fully transform into metakaolin until after the dehydration of the hydroxyl groups was completed. This was evident from the XRD and FTIR analysis [42].

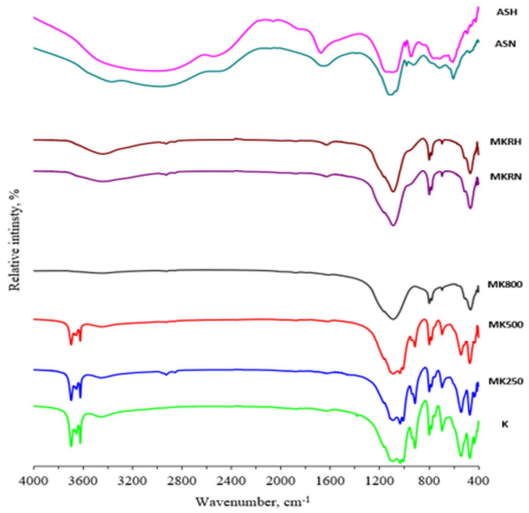

Figure 5: FTIR spectra of kaolin and kaolin calcined at 250-800 ºC (MK250-800), metakaolin residue after dissolution with nitric acid (MKRN) and hydrochloric acid (MKRH), and aluminum sulfate prepared from the dissolution of metakaolin with acids (ASN and ASH).

After calcination up to 800 °C, metakaolin still retained its plate-like morphology, with the onset of agglomeration of the grains because of sintering of MK particles, resulting in larger particle-sized MK grains with a lower surface area [43]. Increasing the calcination temperature disrupts more structures of the $AlO_2(OH)_4$ octahedral layer [44], causing metakaolin particles to separate from the stacked particles and lose their hexagonal structure, as shown in the SEM images. It was clear from the SEM analysis of the residues of dissolving metakaolin with nitric and hydrochloric acids that there was a clear change in the morphological shape of the samples, as they disappeared, which confirms the occurrence of the process of dissolving and dealuminating metakaolin with nitric and hydrochloric acids (Figure 6-MKRN and MKRH). It is clear from the SEM images of the aluminium sulfate samples that the first sample ASN has cubic crystals, while the second sample ASH has leaf-shaped crystals (Figure 6-ASN and ASH).

SEM-EDX analysis (Figure 7) of the residues of dissolving metakaolin with nitric acid (MKRN) and hydrochloric acid (MKRH) showed that the concentration of residual aluminium after dissolution was minimized. This confirms that the process of dissolution and deamination of metakaolin with nitric and hydrochloric acids reached the highest level. The results showed that the prepared aluminium sulfate compounds different in the sodium-to-potassium ratio. The first sample contained potassium, while the second contained sodium.

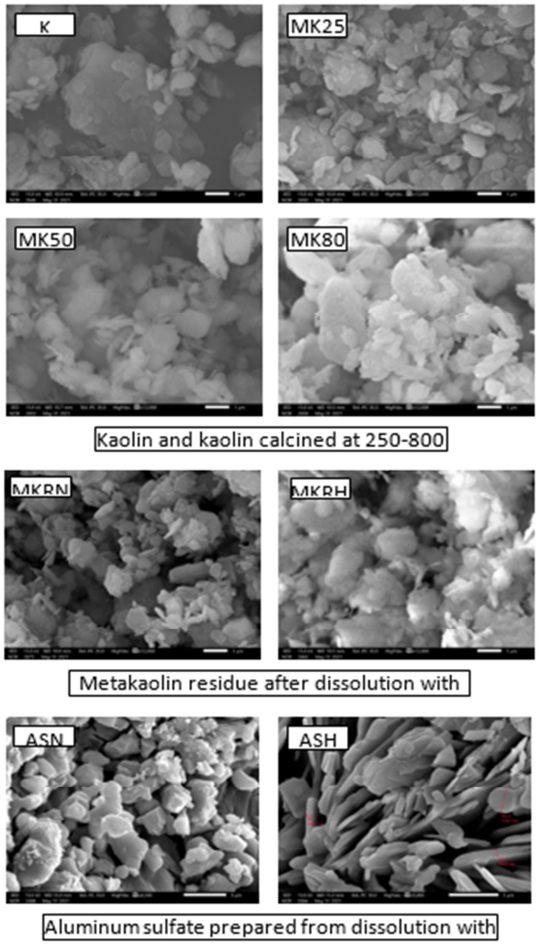

Figure 6: SEM micrographs of kaolin and kaolin calcined at 250-800 ºC (MK250-800), metakaolin residue after dissolution with nitric acid (MKRN) and hydrochloric acid (MKRH), and aluminum sulfate prepared from the dissolution of metakaolin with acids (ASN and ASH).

The results of the elemental analysis of the first compound ASN agree with the approximate molecular formula of the Alum-K mineral, which has the molecular formula $KAl(SO_4)_2.12H_2O$, and the results of the elemental analysis of the second compound ASH agree with the approximate molecular formula of the Tamarugite mineral, which has the molecular formula $NaAl(SO_4)_2.6H_2O$.

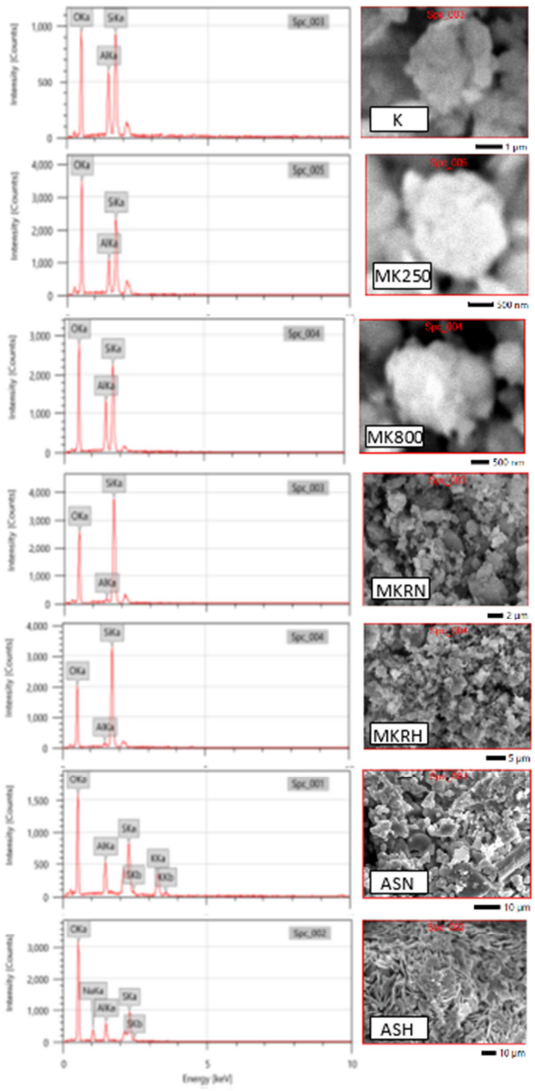

Figure 7: SEM-EDX analysis of kaolin (K) and kaolin calcined at 250-800 ºC (MK250-800), metakaolin residue after dissolution with nitric (MKRN) and hydrochloric acids (MKRH), and aluminum sulfate prepared from dissolution of metakaolin with acids (ASN and ASH).

The TGA analysis of kaolin (Figure 8) shows that a small percentage of weight loss occurs before 200 °C owing to the loss of moisture absorbed by kaolin particles. Then, an accelerated weight loss occurs because of the exit of the water of crystallization [45] after reaching 450 °C and 650 °C because of the partial dihydroxylation of the $AlO_2(OH)_4$ octahedral layer of kaolinite [46]. The rate of weight loss slowed down after reaching 850 °C. The final weight loss at 900 °C is 10.5 wt%. This confirms that the highest rate of exit water of crystallization occurs in the range 450-650 °C and that the choice of burning temperature at 800 °C for the preparation of metakaolin in the following steps is a good choice commensurate with the nature of the kaolin used. It is clear from the TGA analysis of the prepared aluminum sulfate samples that both samples lost approximately 37 % of their weight because of the volatilization of the chemically combined water molecules in the temperature range of 100-350 °C and then underwent a phase of weight stability in the temperature range 350-650 °C and then lost the rest of the water of crystallization in the water at 650-750 °C. The second sample, ASH, also appeared to lose a greater percentage of its weight than the first sample, ASN.

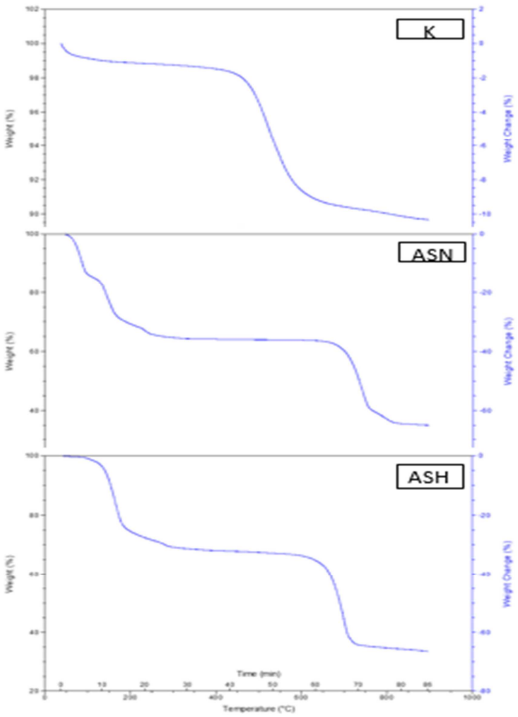

Figure 8: TGA analysis of kaolin (K) and aluminum sulfate prepared by dissolution of metakaolin with acids (ASN and ASH).

Table (2) shows the percentage of extraction of aluminum oxide and iron oxide from metakaolin

using different acids. It is clear from the results that both hydrochloric acid and nitric acid give a relatively close extraction rate in terms of the solubility of aluminum oxide. Hydrochloric acid has a higher extraction rate for iron oxide than nitric acid. This may be because of the calculation of the solubility of these salts. The solubility quotient of iron-(III) chloride may be higher than that of iron (III) nitrate, whereas the solubility quotients of both aluminum nitrate and aluminum chloride are similar.

Table 2: Percentage of extraction of aluminium oxide and iron oxide from metakaolin using different acids

Sample	HNO_3	HCl
Iron oxide extraction, %	69.32	78.46
Aluminium Iron oxide extraction, %	60.88	57.32

Table (3) illustrates the calculations of the molecular formulas and number of chemically combined water molecules for the prepared aluminum sulfate. It is clear from the results that the prepared aluminum sulfate compounds contain 9-10 water molecules, and these results agree with the TGA analysis of the two samples. The various analyses showed complete concordance with the results, which confirmed the results in more than one direction and supported the interpretations and conclusions based on them. The various analyses (TGA, XRD, FTIR, SEM-EDX) showed agreement of the results, which confirms the results in more than one way and supports the interpretations and conclusions based on the research.

Table 3: Calculations of molecular formulas and number of chemically combined water molecules for the prepared aluminium sulfate.

Sample	ASN	ASH
Number of chemically combined water molecules	10	9
Molecular formula	$Al_2(SO_4)_3.10H_2O$	$Al_2(SO_4)_3.9H_2O$
Molecular weight	522	504

Table (4) and Figures (9-11) illustrate the turbidity, residual aluminum, hardness, electrical conductivity, and total dissolved solids of Al Ahsaba dam water and reference drinking water samples after the addition of the prepared and commercial aluminum sulfates. The water sample from the Al Ahsaba dam has an elevated turbidity value in nephelometric turbidity units (NTU). This value increases during a rainy period because the torrential water carries silt particles, fine sand, and suspended materials to the dam reservoir. In addition to the biological activity and decomposition of plant materials and fish waste, the turbidity rates were higher than the calculated value of the water sample. The aluminum salt coagulant provides trivalent aluminum ions that neutralize the suspended negatively charged particles in the water sample, coagulating the neutralized particles and settling by the action of gravity. Accordingly, the turbidity value diminished after the addition of the aluminum salt.

Table 4: Turbidity, residual aluminium, hardness, electrical conductivity, and total dissolved solids of Al Ahsaba dam water and reference drinking water samples after addition of prepared and commercial aluminium sulfates.

No.	Sample	Turbidity, NTU	Residual Al, ppm	H_{tem} ppm	H_{per} ppm	H_{tot} ppm	pH	EC, µS	TDS, ppm
1	W	28.51	4.05	135	83	220	8.55	546	349
2	10ASN	0.66	2.11	125	89	214	8.53	543	348
3	20ASN	0.41	0.81	116	102	218	8.48	557	356
4	30ASN	0.32	1.53	110	104	214	8.54	546	349
5	40ASN	0.21	1.89	107	117	224	8.53	559	358
6	10ASH	1.05	0.97	116	104	220	8.55	544	348
7	20ASH	0.89	0.27	114	108	222	8.50	542	347
8	30ASH	0.74	2.43	113	113	226	8.58	550	352
9	40ASH	0.61	4.21	123	97	220	8.62	548	351
10	10ASR	0.56	2.05	113	109	222	8.60	569	364
11	20ASR	0.23	1.35	105	124	230	8.50	591	378
12	30ASR	0.12	2.43	99	123	222	8.60	622	398
13	40ASR	0.07	3.51	92	136	228	8.53	640	410
14	WR	0.04	41.67	29	45	74	7.66	162	104

The residual Al content depended on the water source. It should be noted that the commercial drinking water sample, which was taken from a groundwater well, contained an aluminium content of the remainder estimated at ten times that of the Al Ahsaba water dam. This is because groundwater dissolves a large amount of aluminium ions because of its exposure to pressure within the aquifers between the layers of rocks. Similarly, the commercial drinking water sample has a low hardness value (approximately one-fourth to one-fifth) compared to the dam's water, as well as electrical conductivity and total dissolved solids (approximately one-third) compared to dam water. However, the amount of residual aluminium increased after the addition of 30 ppm aluminium salt. This, in turn, reduces the usefulness of water because of what may cause an increase in the concentration of aluminium ions to human health.

The aluminium sulfate sample, which was derived from the dissolution of kaolin in nitric acid, retained less residual aluminium than commercial aluminium sulfate even after adding large doses. This is an additional advantage of improving turbidity removal efficiency for less residual aluminium.

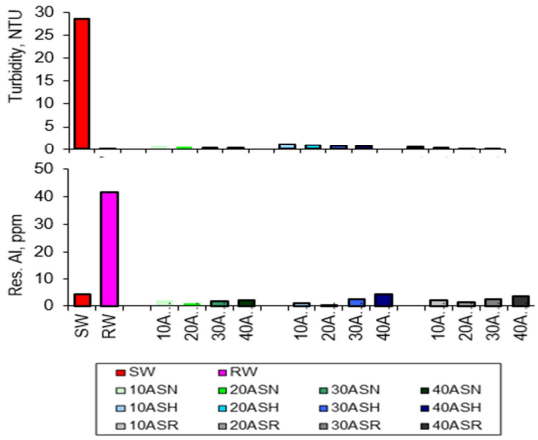

Figure 9: Turbidity (NTU) and residual aluminium (ppm) of Al Ahsaba Dam water and reference drinking water sample after addition of prepared and commercial aluminium sulfates.

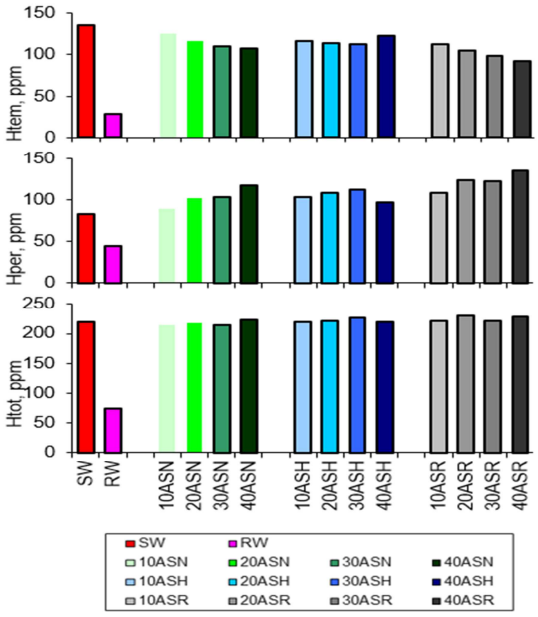

Figure 10: Temporary, permanent, and total hardness (ppm) of Al Ahsaba dam water and reference drinking water sample after the addition of prepared and commercial aluminium sulfates.

It should be noted that the value of the temporary hardness of water, which is caused by calcium and magnesium ions, decreases as the dose of aluminium sulfate increases. The addition of aluminium sulfate reduces the value of the temporary hardness of water owing to the adsorption of calcium and magnesium ions by the accumulated coagulated particles. In contrast, the permanent hardness increased as the dose of aluminium sulfate increased. The addition of aluminium sulfate increased the residual aluminium content, which contributed to the permanent hardness of the water. Therefore, the addition of aluminium sulfate did not change the total hardness of water. Because the addition of aluminium sulfate increased the permanent hardness and reduced the temporary hardness, the total hardness, which is the sum of the two amounts, has a constant value.

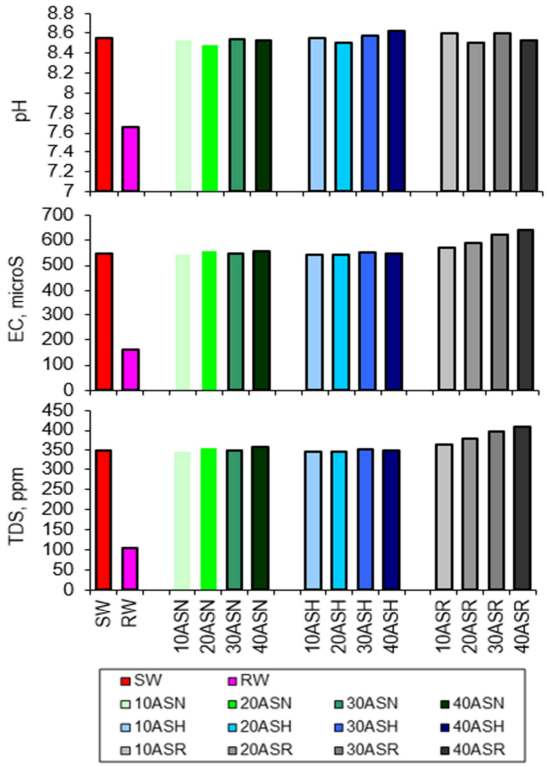

Figure 11: Electrical conductivity, µS and total dissolved solids, ppm of Al Ahsaba dam water, and reference drinking water sample after the addition of prepared and commercial aluminum sulfates.

From the pH measurement, it was noted that the Al Ahsaba dam water sample was slightly alkaline compared to the commercial drinking water sample. The addition of aluminum sulfate does not change the pH of water because aluminum sulfate acts as a buffer [47, 48]. The addition of the prepared aluminum sulfate doses did not change the value of either electrical conductivity or total dissolved solids in water. However, the addition of commercial

aluminum sulfate increased the electrical conductivity and total dissolved solids in water.

4. Conclusions

Amorphous metakaolin was produced by calcination of kaolin at 800 °C. Approximately 60% of alumina was extracted from metakaolin by dissolving it in 8 M hydrochloric and nitric acids at 100 °C. Aluminum sulfate was separated from the acid leaching solution as described in the experimental section.

The chemical composition of dam water is completely different from that of groundwater with respect to the content of dissolved solids, hardness, and pH because of the different environmental factors affecting the water. This was evident in the water samples sample from the Al Ahsaba dam and commercial drinking water.

Measurements proved that aluminum sulfate prepared from kaolin Nawan is similar to commercial aluminum sulfate in its role as a coagulant in turbid water.

When the prepared aluminum sulfate was added to turbid water, the suspended matter precipitated in the form of flocs, which, in turn, caused changes in the chemical composition and physical properties of the water. (1) The turbidity of water diminished. (2) The residual aluminum content increased. (3) The values of the total hardness, pH, electrical conductivity, and total dissolved solids did not change.

Using the prepared aluminum sulfate, it was possible to improve the properties of the dam water sample after removing the turbidity without causing a significant change in the residual aluminum content, hardness, pH, and dissolved solids.

Accordingly, it became possible to supply dam water, after coagulation with the prepared aluminium sulfate, to the same treatment lines in water treatment plants, such as groundwater, until it became suitable for drinking purposes.

5. Conflicts of interest

The authors declare that there are no conflicts to declare regarding to financial interests or personal relationships that could have influenced the work reported in this study.

6. Formatting of funding sources

This work was supported by the Al-Baha University, KSA [grant no. 6-1441].

7. Acknowledgments

The authors would like to acknowledge Al-Baha University for facilitating this study in the laboratories of the Chemistry Department, Faculty of Science and Arts, Mukhwah.

7. References

[1] DeNicola, E., Aburizaiza, O.S., Siddique, A., Khwaja, H., Carpenter, D.O., (2015). Climate change and water scarcity: The case of Saudi Arabia. Annual Global Health, 81, 342-353. http://doi.org/10.1016/j.aogh.2015.08.005

[2] Mahmoud, M.S.A., Abdallh, S.M.A., (2013). Water–Demand Management in the Kingdom of Saudi Arabia for Enhancement Environment. IOSR Journal of Computer Engineering (IOSR-JCE). 14, 2, 57-75. https://doi.org/10.9790/0661-1425775

[3] FAO, (Food and Agriculture Organization)., (2009). Irrigation in the Middle East region in figures. Food and Agriculture Organization of the United Nations. FAO Water Reports 34, Rome.

[4] MOEP, (The Ministry of Economy and Planning)., (2010). The Ninth Development Plan (2010–2014). The Kingdom of Saudi Arabia.

[5] Al-Subaie, F., (2016). The water situation in the Kingdom (7), conclusion. quoted from Al-Iqtisadiah Newspaper. www.aleqt.com

[6] Al-Zahrani, K.H., Al-Shayaa, M.S., Baig, M.B., (2011). Water conservation in the kingdom of Saudi Arabia for better environment: implications for extension and education. Bulgarian Journal Agriculture Science. 17, 389-395.

[7] Chowdhury, S., Al-Zahrani, M., (2013). Implications of climate change on water resources in Saudi Arabia. The Arabian Journal of Science and Engineering. 38, 1959-1971. http://dx.doi.org/10.1007/s13369-013-0565-6

[8] CIA, (2011). CIA Fact Book: Available at: <https://www.cia.gov/library/publications/the-world-factbook/> (accessed 20.09.11).

[9] Sowers, J., Vengosh, A., Weinthal, E., (2011). Climate change, water resources, and the politics of adaptation in the Middle East and North Africa. Climat Change. 104:599-627. https://doi.org/10.1007/s10584-010-9835-4

[10] Saudi Ministry of Water and Electricity., (2011). Dams under Construction in Al Baha, Water Studies Department, Deputy Ministry for Water Affairs, Kingdom of Saudi Arabia.

[11] Aquastat, (2011). Aquastst Geo-referenced database of dams in the Middle East. Avail at: <http://www.fao.org/geonetwork/srv/en/metadata.show?id=38078>.

[12] Argaam, (2018). Saudi Arabia's drinking water consumption rises 8% in 2018, https://www.argaam.com/en/article/articledetail/id/1312492.

[13] Saudi National Water Compan. https://www.nwc.com.sa/English/OurCompany/MediaCenter/NewsandEvents/News/Pages, 2020.

[14] Claverie, M., Martin, F., Tardy, J.P., Cyr, M., De Parseval, P., Grauby, O., Le Roux, C., (2015). Structural and chemical changes in kaolinite caused by flash calcination: formation of spherical particles. Applied Clay Science. 114, 247-255. https://doi.org/10.1016/j.clay.2015.05.031

[15] Rivera, O., Pavez, O., Li Kao, J., Nazer, A., (2016). Metallurgical characterization of kaolin from Atacama, Chile. REM: International

Engineering Journal. 69, 4, 473-478. https://doi.org/10.1590/0370-44672016690005
[16] Al-Nakhebi, Z., Tayeb, O., Bayashoot, A., Al Qurashi, M.M., Al Malhi, M., Al Ahmadi, A., Eskander, N., (2007). Exploration of kaolinitic clay deposits in the south Jabal Shahbah area, Kingdom of Saudi Arabia. Saudi Geological Survey Open-File Report SGS-OF-2006-4, 35p.
[17] Mohsen, Q., El-maghraby, A., (2010). Characterization and assessment of Saudi clays raw material at different area. Arabian Journal of Chemistry. 3, 271-277. https://doi.org/10.1016/j.arabjc.2010.06.015
[18] Ramasamy, S., Abdullah, M.M.A., Huang, Y., Hussin, K., Wang, J., Shahedan, N.F., (2017). Correlation between Hardness and Water Absorption Properties of Saudi Kaolin and White Clay Geopolymer Coating. American Institute of Physics Conference Proceedings. 1885:020224. https://doi.org/10.1063/1.5002418
[19] Eren, E., (2008). Removal of copper ions by modified unye clay, Turkey. Journal of Hazardous Materials. 159, 2-3, 235-244. https://doi.org/10.1016/j.jhazmat.2008.02.035
[20] Dogan, M., Turhan, Y., Alkan, M., Namli, H., Turan, P., Demirbas, O., (2008). Functionalized sepiolite for heavy metal ions adsorption. Desalination. 230, 1-3, 248-268. https://doi.org/10.1016/j.desal.2007.11.029
[21] Alandis, N.M., Mekhamer, W., Aldayel, O., Hefne, J.A.A., Alam, M., (2019). Adsorptive Applications of Montmorillonite Clay for the Removal of Ag(I) and Cu(II) from Aqueous Medium. Journal of Chemistry. Article ID 7129014. 2019:7p. https://doi.org/10.1155/2019/7129014
[22] Al-Sawalha, M., Ratemi, E., (2018). Properties of Raw Saudi Arabian Grey Kaolin Studied by Pyrrole Adsorption and Catalytic Conversion of Methylbutynol. Journal of Chemistry. Article ID 8656207. 2018:6P. https://doi.org/10.1155/2018/8656207
[23] Tantawy, M.A., Alomari, A.A., (2019). Extraction of Alumina from Nawan Kaolin by Acid Leaching. Oriental Journal of Chemistry. 35, 3, 1013-1021. https://doi.org/10.13005/ojc/350313
[24] Saritha, V., Karnena, M.K., Dwarapureddi, B.K., (2019). Exploring natural coagulants as impending alternatives towards sustainable water clarification" – A comparative studies of natural coagulants with alum. Journal of Water Process Engineering. 32, 100982 (14p), https://doi.org/10.1016/j.jwpe.2019.100982
[25] Gandiwa, B.I., Moyo, L.B., Ncube, S., Mamvura, T.A., Mguni, L.L., Hlabangana, N., (2020). Optimization of using a blend of plant based natural and synthetic coagulants for water treatment: (Moringa Oleifera-Cactus Opuntia-alum blend). South African Journal of Chemical Engineering. 34, 158-164. https://doi.org/10.1016/j.sajce.2020.07.005
[26] Pehlivan, A., Aydin, A.O., Alp, A., (2012). Alumina extraction from low grade diasporic bauxite by pyro-hydro metallurgical process. SA¨U Fen Bilimleri Enstit¨us¨u Dergisi, 16, 2, 92-987. https://doi.org/10.5505/saufbe.2012.73645
[27] Al-Zahrani, A.A., Abdul-Majid, M.H., (2009). Extraction of alumina from local clays by hydrochloric acid process. JKAU: Engineering Science. 20, 2, 29-41. https://doi.org/10.4197/Eng.20-2.2
[28] Chigondo, F., Nyamunda, B.C., Bhebhe, V., (2015). Extraction of Water Treatment Coagulant from Locally Abundant Kaolin Clays. Journal of Chemistry. Article ID 705837. 2015:7p. https://doi.org/10.1155/2015/705837
[29] Al-Zahrani, A.A., Abdul-Majid, M.H., (2004). Production of liquid alum coagulant from local Saudi clays. JKAU: Engineering Science. 15, 1, 3-17. https://doi.org/10.4197/Eng.15-1.1
[30] Al-Zahrani, A., Al-Zaitone, B., (2017). Production of alumina from Saudi clay by sulfuric acid leaching. International Journal of Engineering Sciences and Research Technology. 6, 2, 285-293.
[31] Al-Jlil, S.A., (2017). Adsorption of cobalt ions from waste water on activated Saudi clays. Applied Water Science. 7, 383-391. https://doi.org/10.1007/s13201-014-0253-z
[32] Jeffery, G.H., Bassett, J., Mendham, J., Denney, R.C., (1989). Vogel's textbook of quantitative chemical analysis, 5th edition, Longman scientific and technical group, UK.
[33] El-Ouatib, R., Guillemet, S., Durand, B., Samdi, A., Rakho, L.E., Moussa, R., (2005). Reactivity of aluminum sulfate and silica in molten alkali-metal sulfates in order to prepare mullite. Journal of European Ceram Society. 25, 1, 73-80. https://doi.org/10.1016/j.jeurceramsoc.2003.12.002
[34] Eisazadeh, A., Kassim, K.A., Nur, H., (2012). Solid-state NMR and FTIR studies of lime stabilized montmorillonitic and lateritic clays. Applied Clay Science. 67, 68, 5-10. https://doi.org/10.1016/j.clay.2012.05.006
[35] Frost, R.L., Kristof, J., Paroz, G.N., Tran, T.H., Kloprogge, J.T., (1998). The role of water in the intercalation of kaolinite with potassium acetate. Colloid International Science. 204, 227-236. https://doi.org/10.1006/jcis.1998.5604
[36] Zhang, D., Pan, X., Yu H., Zhai, Y., (2015). Mineral transition of calcium aluminate clinker during high-temperature sintering with low-lime dosage. Journal of Material Science. Technol. 31, 1244-1250. https://doi.org/10.1016/j.conbuildmat.2012.09.071
[37] Madejova, J., Komadel, P., (2001). Baseline studies of the clay minerals society source clays: infrared methods. Clay Minerals. 49, 410-432. https://doi.org/10.1346/CCMN.2001.0490508
[38] Lecomte, I., Liégeois, M., Rulmont, A., Cloots, R., Maseri, F., (2003). Synthesis and characterization of new inorganic polymeric composites based on kaolin or white clay and on ground-granulated blast furnace slag. Journal of Material Research. 18, 2571-2579. https://doi.org/10.1557/JMR.2003.0360
[39] China, C.R., Hilonga, A., Maguta, M.M., Nyandoro, S.S., Kanth, S.V., Jayakumar, G.C.,

Njau, K.N. (2019). Preparation of aluminum sulphate from kaolin and its performance in combination tanning. SN Applied Sciences. 1, 920-927. https://doi.org/10.1007/s42452-019-0979-1

[40] Sangita, S., Nayak, N., Panda, C.R., (2017). Extraction of aluminum as aluminum sulphate from thermal power plant fly ashes, Transactions of Nonferrous Metals Society of China. 27, 2082-2089. https://doi.org/10.1016/S1003-6326(17)60231-0

[41] Aderemi, B.O., Hameed, B.H., (2009). Alum as a heterogeneous catalyst for the transesterification of palm oil. Applied Catalysis A: General. 370, 1-2, 54-58. https://doi.org/10.1016/j.apcata.2009.09.020

[42] Wang, M., Guo, N., He, P., Yu, J., Jia, D., (2014). Formation Mechanism and Its Pozzolanic Activity of Metakaolin. Key Engineering Materials. 602-603, 620-623. https://doi.org/10.4028/www.scientific.net/KEM.602-603.620

[43] Fabbri, B., Gualtieri, S., Leonardi, C., (2013). Modifications induced by the thermal treatment of kaolin and determination of reactivity of metakaolin. Applied Clay Science. 73, 2-10.

[44] Peng, H., Vaughan, J., Vogrin, J., (2018). The effect of thermal activation of kaolinite on its dissolution and re-precipitation as zeolites in alkaline aluminate solution. Applied Clay Science. 157, 189-197. https://doi.org/10.1016/j.clay.2018.03.002

[45] Zhang, Y., Xu L., Seetharaman, S., Liu, L., Wang, X., Zhang, Z., (2015). Effects of chemistry and mineral on structural evolution and chemical reactivity of coal gangue during calcination: towards efficient utilization. Material Structure. 48, 2779-2793. https://doi.org/10.1617/s11527-014-0353-0

[46] Xu, X.H., Lao, X.B., Wu, J.F., Zhang, Y.X., Xu, X.Y., Li, K., (2015). Microstructural evolution, phase transformation, and variations in physical properties of coal series kaolin powder compact during firing. Applied Clay Science. 115, 76-86. https://doi.org/10.1016/j.clay.2015.07.031

[47] Williams, D.J., Creasy, W.R., McGarvey, D.J., Fry, R.A., Bevilacqua, V.L.H., Durst H.D., (2009). Aluminum sulfate and sodium aluminate buffer solutions for the destruction of phosphorus based chemical warfare agents. New Journal of Chemistry. 33, 1006-1009. https://doi.org/10.1039/B819885C.

[48] Burdock, G., (1997). Encyclopedia of food and color additives. CRC Press. https://doi.org/10.1201/9781498711081